



Knockdown of Pim-3 Suppresses the Tumorigenicity of Glioblastoma by Regulating Cell Cycle and Apoptosis

J. Quan, L. Zhou and J. Qu^{*}

Department of Neurosurgery, The Second Affiliated Hospital of Xi'an Jiao Tong University, Xi'an, 710004, Shanxi, China

Corresponding author: Jianqiang Qu, Department of Neurosurgery, The Second Affiliated Hospital of Xi'an Jiao Tong University, Xi'an, 710004, Shanxi, China. Email: lxgang_lxg@163.com

Abstract

Products of the Pim (the proviral integration site for the Moloney murine leukemia virus) family of proto-oncogenes possess serine/threonine kinase activity and belong to the Ca²⁺/calmodulin-dependent protein kinase group. Pim-3, a member of the Pim family is closely linked to the development of a variety of tumors. However, the role of Pim-3 in human glioblastoma remains unknown. In this study, we elucidated the role of Pim-3 in the growth and apoptosis of glioblastoma cells. Western blotting was used for determination of protein levels, and shRNA was used for Pim-3 knockdown. The MTT assay was used to evaluate cell proliferation and flow cytometry was used to determine cell cycle status and the number of apoptotic cells. A mouse xenograft model was established by injecting nude mice with Pim-3-depleted glioblastoma cells in order to determine tumor growth *in vivo*. We demonstrated that Pim-3 was highly expressed in human glioblastoma cell lines. We also found that knockdown of Pim-3 by specific shRNA slowed decreased proliferation, induced cell cycle arrest in the G0/G1 phase, and increased apoptosis in glioblastoma cells. Pim-3 knockdown potently inhibited the growth of subcutaneously implanted glioblastoma cells *in vivo*. We further revealed that Pim-3 knockdown induced growth inhibition by reducing the levels of the anti-apoptotic protein Bcl-xl and cell cycle regulatory proteins, including cyclin D1 and Cdc25C, and increasing the levels of the pro-apoptotic protein Bax.

Key words: Pim-3, glioblastoma, shRNA, cell cycle, apoptosis.

Introduction

Glioblastoma is one of the most common types of brain tumor (1, 2). Glioblastoma multiforme are grade IV astrocytic brain tumors, based on their histopathological features and clinical presentation (3). Although, there are diverse therapeutic modalities such as surgery, radiation, and chemotherapy, the prognosis of patients with glioblastoma is discouraging, with a median survival time of 12-15 months (4). Many cellular dysfunctions such as increased cell proliferation, diffuse infiltration, and high resistance to apoptosis contribute to the high malignancy of glioblastoma (5-7). Therefore, a better understanding of the molecular mechanisms underlying cellular survival and apoptosis resistance may facilitate the development of novel adjuvant therapeutics for improving glioblastoma treatments.

Gene therapy strategies based on the delivery and expression of therapeutic genes, which can inhibit tumor growth and induce tumor cell death, are being very actively pursued (8). Mutation of p53 is the most frequently found genetic mutation in human glioma. Delivering normal p53 into glioma cells potently inhibits tumor growth and triggers apoptosis (9). Gene therapy strategies for the treatment of malignant gliomas continue to be studied in animal models despite their generally unsatisfactory therapeutic effects (10, 11). However, the abortive trials of gene therapy for glioblastoma have necessitated attempts to find novel therapeutic molecules that are more specifically involved in glioblastoma. The proto-oncogene Pim-3 (the proviral integration site for the Moloney murine leukemia virus-3) has been reported to be closely related to a variety of human tumors because of the serine/threonine kinase activity and Ca²⁺/

calmodulin-dependent protein kinase activity of its protein product (12). As a member of the Pim family, Pim-3 shares structural similarity with Pim-1. Since most tumor growth shows the inhibition of apoptosis, the role of Pim-3 in human tumor growth is invariably associated with pro-apoptotic/anti-apoptotic imbalances. It has been reported that aberrant expression of Pim-3 results in phosphorylation of the serine residue of pro-apoptotic Bad, leading to the inactivation of Bad and inhibition of apoptosis in human pancreatic cancer cells (13). In addition, Pim-3 can be induced by ETS-1 (protein C-ets-1), a transcription factor that binds to the promoter of the human *Pim-3* gene, a mechanism that prevents apoptosis in human pancreatic cancer cells (14). Likewise, Pim-3 positively regulates STAT3 (signal transducer and activator of transcription 3) signaling through phosphorylation, whereas Pim-3 inhibitors cause growth inhibition of prostate cancer cells by downregulating the expression of pSTAT3 (Tyr705) (15). In transgenic mice that express Pim-3 exclusively in the liver, Pim-3 was shown to accelerate hepatocellular carcinoma (HCC) development when induced by a hepatocarcinogen, such as diethylnitrosamine (DEN) (16). Pim-3 is also found to be associated with human colon cancer through inactivation of Bad by phosphorylation of Ser112, thereby preventing apoptosis and promoting the progression of HCC (17). Moreover, studies also indicated that Pim-3 could promote angiogenesis in primary human tumors *in vitro* and *in vivo* in mouse models (18, 19). Together, these reports indicate that the role of Pim-3 in human tumor development might be related to its function in regulating apoptosis-related proteins. These studies of Pim-3 have also raised our interest as to whether Pim-3 plays a pivotal role in human glioblastoma

development.

In the present study, we focus on elucidating the role of Pim-3 in the growth and apoptosis of glioblastoma cells. We determined the expression level of Pim-3 in human glioblastoma cell lines. In addition, through both *in vitro* and *in vivo* analysis, we attempted to identify the possible mechanisms that could contribute to Pim-3-regulated glioblastoma development.

Materials and methods

Cell lines and cell culture

The three-glioblastoma cell lines U87MG, U87, and U251 were obtained from the American Type Culture Collection (ATCC, Manassas, VA, USA). All cell lines were cultured in Dulbecco's modified Eagle medium (DMEM, Gibco) supplemented with 10% fetal bovine serum (FBS, Gibco), 10 units/mL penicillin and 10 mg/mL streptomycin (1% penicillin/streptomycin, Thermo Scientific HyClone) at 37°C in a humidified incubator with 5% CO₂.

Construction of recombinant lentivirus

To stably deplete from the glioblastoma cells of Pim-3, a small interfering RNA (siRNA) targeting human Pim-3 was synthesized with the sense sequence of 5'-GGCGUGCUUCUCUACGAUATT-3' and inserted into the pFH-L plasmid (Hollybio, Shanghai, China). The non-silencing siRNA (siCon, 5'-TTCTCCGAA-CGTGTCACGT-3') was used as a control. The lentivirus-based short hairpin RNA (shRNA)-expressing vectors were confirmed by DNA sequencing and named as shPim-3 or shCon. Recombinant pFH-L plasmid together with the two packaging plasmids was co-transfected into 293T cells using Lipofectamine 2000 (Invitrogen, Carlsbad, CA, USA) according to the manufacturer's instructions. The supernatant was collected 48 h after transfection, centrifuged (4000 g, 10 min, 4°C), and filtered through 0.45 µm filters. The titer of concentrated lentivirus was determined by dilution and using fluorescent microscopy.

Lentivirus infection

U87 and U251 cells (3 × 10⁴) were seeded in 6-well plates prior to infection with lentivirus-shPim-3 (Lv-sh-Pim-3) or lentivirus-shCon (Lv-shCon) at a multiplicity of infection (MOI) of 50. As the lentivirus carries green fluorescence protein (GFP), the infection efficiency was determined by counting GFP-expressing cells under fluorescence microscopy 96 h after infection.

RNA extraction and Quantitative real-time PCR (qRT-PCR)

Total RNA of cultured U87 and U251 cells (Con group, Lv-shCon group, Lv-shPim-3 group) was extracted using the Trizol solution (Invitrogen, Carlsbad, CA). The isolated RNA was immediately converted to cDNA by reverse transcription using the SuperScript III First-Strand Synthesis System (Invitrogen, Carlsbad, CA). Then, by using the SYBR Premix Ex Taq™ Perfect Real Time (TaKaRa, Shiga, Japan), the mRNA level of Pim-3 was evaluated by real-time PCR on an ABI PRISM 7500 Real-Time System. β-Actin was used as the input reference. The primers' sequences are as

follows:

Pim-3: Forward, 5'-AAGGACGAAAATCTGCTTG-TGG-3' Reverse, 5'-CGAAGTCGGTGTAGACCG-TG-3'

β-actin: Forward, 5'-GTGGACATCCGCAAAGAC-3' Reverse, 5'-AAAGGGTGTAAACGCAACTA-3'

Relative mRNA level was determined by using the formula $2^{-\Delta\Delta CT}$ (CT; cycle threshold) where $\Delta\Delta CT = CT$ (target gene) - CT (β-actin).

Western blot

Glioblastoma cells were lysed and sonicated in a lysing buffer complemented by protease inhibitors (Chemicon Millipore, Billerica, MA, USA). Total protein concentrations of samples were determined using the BCA Protein Assay Kit (Pierce, Rockford, IL). Primary antibodies used for western blot analysis were rabbit anti-human Cdc25C antibody (1:1000; Santa Cruz, CA), rabbit anti-human Bax antibody (1:1500; CST), rabbit anti-human Bcl-xl antibody (1:1500; CST), rabbit anti-human Cyclin D1 antibody (1:1000; Millipore), rabbit anti-human Pim-3 antibody (1:1000; Abcam), rabbit anti-human glyceraldehyde 3-phosphate dehydrogenase (GAPDH; 1:5000; Millipore) and rabbit anti-human β-actin (1:5000; Santa Cruz, CA). Horseradish peroxidase (HRP)-conjugated second antibodies were used (1:4000; Santa Cruz) and immunoreactivity was detected with enhanced chemiluminescent autoradiography (ECL kit, Amersham). The expression levels of each sample were quantified using NIH ImageJ software.

MTT assay

The 3-(4,5-dimethylthiazol-2-yl)-2,5-diphenyltetrazolium bromide (MTT) colorimetric assay was used to determine glioblastoma cell proliferation. Lv-shPim-3-infected U87 and U251 cells were seeded in 96-well plates (1 × 10⁴ cells/well) and cultured for five days at 37°C and 5% CO₂. U87 and U251 cells that were treated with vehicle only (Lipofectamine 2000) or Lv-shCon were used as controls. At each time point, 10 µL of the MTT reagent (5 mg/mL in PBS) were added to each well. The reaction was terminated by addition of 100 µL of dimethyl sulfoxide (DMSO; Sigma) after four hours of incubation at 37°C. The optical density (OD) was determined by measuring absorbance at a wavelength of 570 nm. Data presented here were obtained from six independent tests.

Fluorescence-activated cell sorting analysis (FACS)

Cell cycle analysis was performed by staining DNA content with propidium iodide (PI). Briefly, U87 and U251 cells (Con group, Lv-shCon group, and Lv-sh-Pim-3 group) were harvested at 95% confluency. Cells of each group were washed with ice-cold PBS (phosphate buffered saline) and then fixed in 70% ethanol at 4°C for at least 1 h. After fixation, cells of each group were washed twice with PBS, and then incubated with 10 mg/mL RNase A (MBI Fermentas) and 50 mg/mL PI (Sigma) for 30 min in the dark. The percentage of cells in different phases of the cell cycle was analyzed by a flow cytometer (FACS Calibur, BD Biosciences).

For apoptosis analysis, three groups of U87 and U251 cells were harvested and incubated with fluores-

cein isothiocyanate (FITC)-conjugated Annexin V and propidium iodide (PI) according to the manufacturer's protocol (BD Biosciences). Then, the suspension was filtered through a 50- μm nylon mesh, and 10^4 stained cells were analyzed by a flow cytometer (FACS Calibur, BD Biosciences).

Morphological examination for apoptosis

U87 and U251 cells (Con group, Lv-shCon group, and Lv-shPim-3 group) were seeded on slides at a density of $3 \times 10^4/\text{mL}$ in six-well plates and cultured for 24 h. Subsequently, the cells were washed three times with PBS and fixed in 4% paraformaldehyde for 10 min. Then, cells were stained with Hoechst 33258 (Sigma) for 5 min, and observed under a fluorescence microscope. The nuclei of the living cells were a homogeneous blue; those of apoptotic cells were compact, condensed, and whitish-blue.

Tumor xenograft assay

To investigate the effect of Pim-3 on the tumorigenesis of glioblastoma cells, a glioblastoma xenograft was established in nude mice. Twenty female Balb/C athymic nude mice (five weeks old) were purchased from the Shanghai Laboratory Animal Center, Chinese Academy of Sciences (SLACCAS) and housed in specific pathogen free (SPF) condition. Mice were divided into Lv-shCon group and Lv-shPim-3 group ($n = 10$ for each group). For each group of mice, both U87 and U251 cells that received corresponding lentivirus infection were used and injected subcutaneously into the right flank of the nude mice (0.2 mL single-cell suspension for each mouse). All procedures were performed on nude mice according to the official recommendations of Chinese Community Guidelines. The maximum diameter (a) and minimum diameter (b) were measured with calipers twice a week. The tumor volume was calculated by the following formula: $V (\text{cm}^3) = \frac{1}{6} \pi ab^2$. All

mice were sacrificed by cervical dislocation on day 28. All efforts were made to minimize the suffering of the animals in this study.

Statistical analysis

Data were analyzed using GraphPad Prism software version 6.00 for Windows (GraphPad Prism Software, San Diego, CA, USA). Average values were expressed as mean \pm standard deviation (SD). Statistical significance between different groups was determined by a repeated-measures ANOVA test and P value < 0.05 was accepted as statistically significant.

Results

Expression profile of Pim-3 in human glioblastoma cell lines

To investigate the role of Pim-3 in glioblastoma, we first assessed the expression levels of Pim-3 in three human glioblastoma cancer cell lines, including U87MG, U87, and U251. As shown in Fig. 1A, Pim-3 was highly expressed in all three glioblastoma cell lines, and showed the highest levels in U87 and U251 cells, making these two cell lines ideal for subsequent investigations. We also assessed expression levels of other Pim family members in glioblastoma cells; only Pim-3 shows high expression as compared to Pim1 and Pim2 (Fig. 1B).

Specific and effective down-regulation of Pim-3 in glioblastoma cells by lentivirus-delivered siRNA against Pim-3

In order to further explore the role of Pim-3 in glioblastoma cells, U87 and U251 cells were infected with lentivirus expressing Pim-3 specific siRNA (Lv-shPim-3) and GFP. The efficiency of lentiviral vector transduction in U87 and U251 cells was examined 96 h post-transduction by fluorescent microscopy, and about 70% of the cells were infected with Lv-shCon or Lv-shPim-3 at a MOI of 50 as indicated by the expression of GFP (Fig. 2A). To determine the knockdown potency, qRT-PCR was performed to determine the transcription level of Pim-3. As shown in Fig. 2B, mRNA levels of Pim-3 in the control group and Lv-shCon group showed similar results. However, mRNA levels of Pim-3 in both U87 and U251 cells infected with Lv-shPim-3 were significantly reduced by more than 80%. In addition, to examine the effect of shRNA on Pim-3 protein levels, western blotting was performed in both U87 and U251 cells. As shown in Fig. 2C, in U87 and U251 cells, only weak bands were detected in glioblastoma cells infected with Lv-shPim-3, while strong bands were observed in both Con group and Lv-shCon group cells. Moreover, the shRNA targeting Pim-3 did not recognize the sequences of Pim-1 or Pim-2 (Fig. 2D), indicating the specific knockdown of Pim-3 by our designed shRNA. These results indicated that lentivirus-mediated delivery of shRNA against Pim-3 effectively and specifically inhibited the expression of Pim-3 in glioblastoma cells.

Growth inhibition of glioblastoma cells due to knockdown of Pim-3

To determine the effect of Pim-3 knockdown by RNAi on the growth of glioblastoma cells, MTT assays

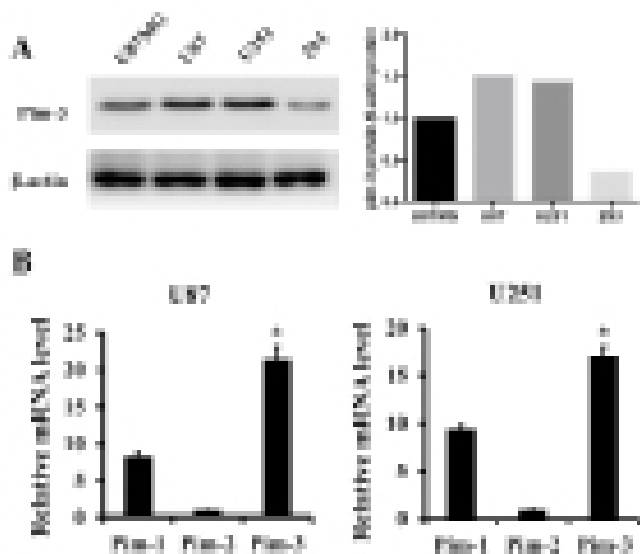


Figure 1. Basal Pim-3 expression in three different glioblastoma cell lines. (A) Western blot analysis showed that Pim-3 was highly expressed in U87MG, U87, and U251 glioma cells; the expression levels of Pim-3, and β -actin were quantified using NIH ImageJ software, Pim-3/ β -actin ratios were calculated for each cell line; the expression levels in U87 and U251 cells were higher than in U87MG cells. (B) Pim-3 had a higher expression level than Pim-1 and Pim-2 in the examined cells.

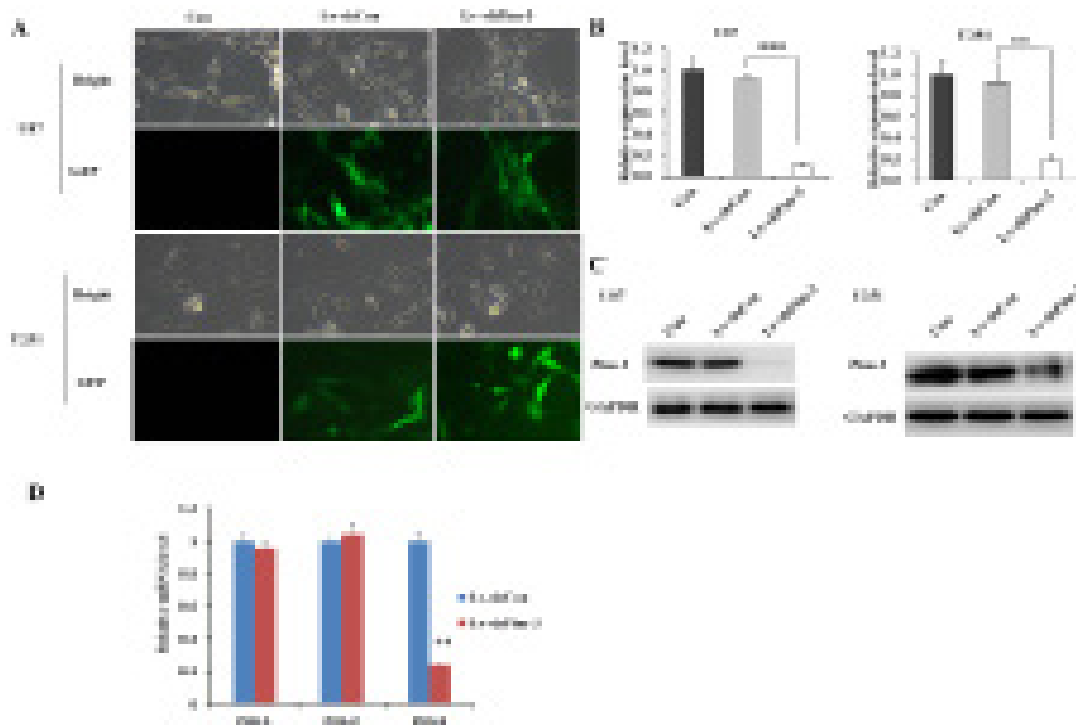


Figure 2. Efficient inhibition of Pim-3 expression by infection with Lv-shPim-3 in glioblastoma cells. (A) Infection was observed to be efficient at 96 h, with over 70% U87 and U251 cells GFP positive in both the Lv-shCon and Lv-shPim-3 groups. (B) qRT-PCR data showing strong Pim-3 mRNA depletion in glioblastoma cells infected with Lv-shPim-3 compared to control cells infected with a scrambled sequence (Lv-shCon). (C) Western blot analysis showing efficient inhibition of Pim-3 protein expression in U87 and U251 cells infected with Lv-shPim-3. (D) Expression levels of Pim-1 and Pim-2 were not altered by the shRNA against Pim-3 in U251 cells. **, $P < 0.01$, ***, $P < 0.001$.

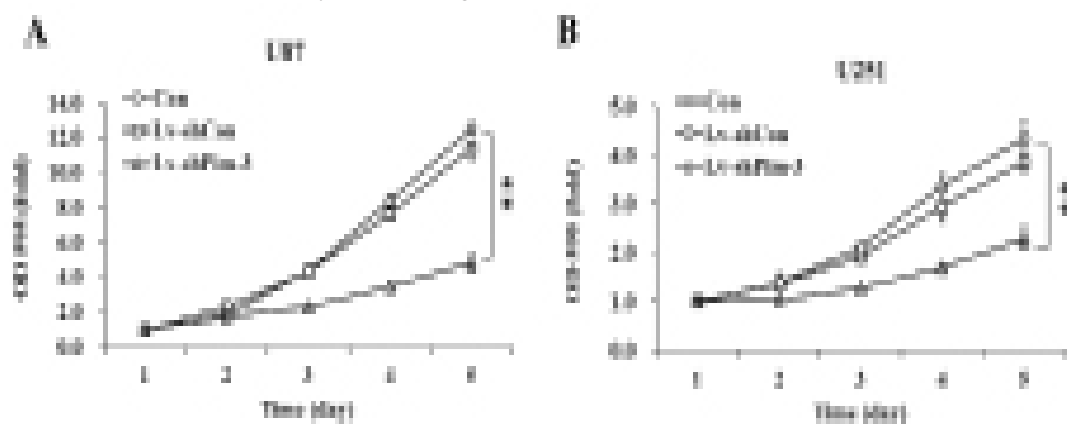


Figure 3. Pim-3 inhibition suppresses glioblastoma cell proliferation. A proliferation assay performed with U87 cells (A) and U251 cells (B) showed a significant decrease in cell number when cells were infected with Lv-shPim-3 compared to uninfected and Lv-shCon infected U87 cells on day five, as demonstrated by MTT assay. Data are presented as mean \pm SD, ** $P < 0.001$.

were performed on glioblastoma cell lines U87 and U251 cells. Cell proliferation was measured daily for five consecutive days. As shown in Fig. 3A, the proliferation rate of U87 cells was significantly decreased by 54.4% on day four and even by 57.5% by day five when these cells were depleted of Pim-3. Comparable results were observed in Lv-shPim-3-infected U251 cells which reductions in proliferation of 42.3% on day four and 40.9% on day five (Fig. 3B). These results suggested that knockdown of Pim-3 in both U87 cells and U251 cells led to significant inhibition of cell proliferation in a time-dependent manner.

Pim-3 knockdown-induced cell cycle arrest in glioblastoma cells

To further explore the mechanism underlying the inhibition of cell proliferation, we examined the effects of Pim-3 knockdown on cell cycle progression in U87 and U251 cells. As shown in Fig. 4A and 4B, compared

with the Lv-shCon group of U87 cells, the percentage of cells in G0/G1 phase in the Lv-shPim-3 group was increased by 10%, whereas the percentage of S-phase was significantly reduced by 9.2%. Similarly, compared with the Lv-shCon group of U251 cells, the percentage of cells in G0/G1 phase in the Lv-shPim-3 group was increased by 11.2%, whereas the percentage of S-phase was significantly reduced by 7.5% (Fig. 4A and 4B). These results indicate that Pim-3 knockdown resulted in cell cycle arrest, with a greater proportion of cells in G0/G1 phase and a concomitant reduction of the cell population in S-phase, which may explain the inhibition of glioblastoma cell proliferation.

Pim-3 knockdown-induced apoptosis in glioblastoma cells

The G0/G1 phase is a crucial checkpoint for DNA damage, and cell cycle arrest at this point is always associated with apoptosis (20). Therefore, we assessed

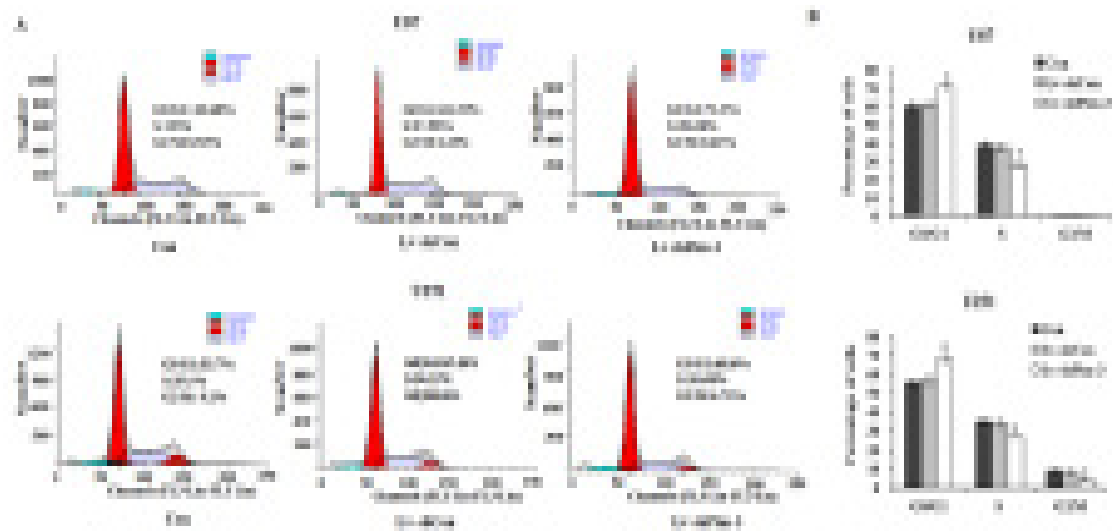


Figure 4. Pim-3 inhibition regulated cell cycle of U87 and U251 cells *in vitro*. (A) Cell cycle analysis by flow cytometry of U87 and U251 cells in three distinct groups (Con, Lv-shCon, and Lv-shPim-3). (B) Percentage of cells in distinct cell cycle stages of three distinct groups (Con, Lv-shCon, and Lv-shPim-3) in U87 and U251 cells. Data are presented as mean \pm SD, n = 3; *P < 0.05.

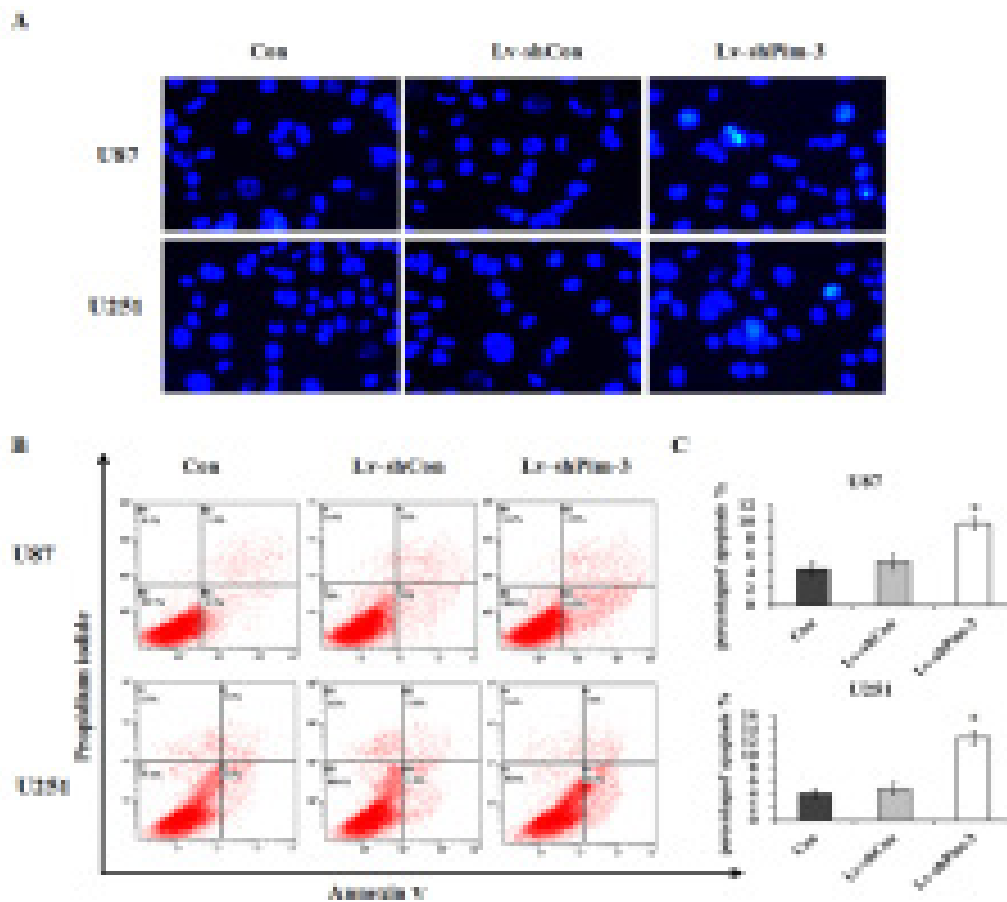


Figure 5. Pim-3 inhibition induced potent apoptosis in glioblastoma cells. (A) Morphological apoptosis was determined in two glioblastoma cell lines (U87 and U251) by staining with Hoechst 33258. (B) Dot plot representing the percentage of Annexin V-positive cells in U87 and U251 cultures analyzed by flow cytometry and Annexin V-FITC and propidium iodide (PI) staining. (C) Quantification of Annexin V-FITC positive and PI negative cells. Pim-3 inhibition (Lv-shPim-3) resulted in a significant increase in early apoptotic cells. Data are presented as mean \pm SD, n = 3; *P < 0.05 compared with the Lv-shCon infected groups.

the effect of Pim-3 knockdown on apoptosis in U87 and U251 cells. Hoechst 33258, a DNA-sensitive fluorochrome, was used to detect changes in the nuclear morphology of glioblastoma cells after Pim-3 knockdown. As shown in Fig. 5A, the nuclei in uninfected cells or Lv-shCon infected U87 and U251 cells exhibited diffuse staining of the chromatin. However, Lv-shPim-3 infected U87 and U251 cells showed chromatin condensation, margination, and shrunken nuclei, which are indicative of apoptosis. To further determine the effects

of Pim-3 on apoptosis, cells from distinct groups were stained with Annexin V and PI for detection of apoptosis. As shown in Fig. 5B and 5C, the percentages of the early stage of apoptosis detected by Annexin V-FITC were 4.5%, 5.2%, and 9.2% in uninfected, Lv-shCon infected, and Lv-shPim-3 infected U87 cells, respectively. Correspondingly, the percentages of cells in the early stages of apoptosis, detected by Annexin V-FITC, were 4.0%, 4.6%, and 12.6% in uninfected, Lv-shCon-infected, and Lv-shPim-3-infected U251 cells, respectively.

These results show that Pim-3 influenced apoptosis of glioblastoma cells *in vitro*, providing further evidence of the involvement of Pim-3 in promoting proliferation of glioblastoma cells.

Tumor xenograft growth inhibition *in vivo* due to Pim-3 knockdown

To determine whether Pim-3 affected glioblastoma progression *in vivo*, a murine xenograft model was established. The right flank of nude mice was subcutaneously injected with U87 and U251 cells that were infected with Lv-shCon or Lv-shPim-3 ($n = 5$ for each group in each cell line). As illustrated in Fig. 6A, in U87 cells, tumors grow progressively in the control group. However, tumor size was significantly smaller than the age-matched control mice at day 20 (upper panel). At day 27, tumors were dissected and tumor size was confirmed to be significantly smaller in the Lv-shPim-3 group (lower panel). Similar results were also obtained from U251 cells (Fig. 6B). Moreover, we performed immunohistochemistry analysis of the apoptosis-related factors Bax and Bcl-xl in the tumor tissues. It was shown that pro-apoptotic Bax was increased whereas anti-apoptotic Bcl-xl was decreased in the Lv-shPim-3 groups in both U87 cells and U251 cells (Fig. 6C). These results suggested that Pim-3 knockdown inhibited the growth of subcutaneously implanted glioblastoma tumors *in vivo*.

Regulation of cell cycle- and apoptosis-related proteins due to Pim-3 knockdown in glioblastoma cells

Herein, the expression levels of the cell cycle-related proteins cyclin D1 and Cdc25C and the apoptosis-related proteins Bcl-xl and Bax were analyzed by western blot in uninfected, Lv-shCon infected, and Lv-shPim-3 infected U87 and U251 cells. As shown in Fig. 7, the levels of Bcl-xl, Bax, cyclin D1, and Cdc25C in uninfected cells and Lv-shCon infected cells were relatively consistent. However, the pro-apoptotic protein Bax increased significantly in response to Pim-3 knockdown in the Lv-shPim-3 infected cells. On the contrary, anti-apoptotic protein Bcl-xl and cell cycle regulatory proteins including cyclin D1 and Cdc25C decreased dramatically in Lv-shPim-3 infected cells. The above data indicate that Pim-3 knockdown inhibits proliferation, at least partially, by modulating expression of these apoptosis-related proteins and cell cycle regulatory proteins in the glioblastoma cells.

Discussion

Pim-3 was originally identified as the depolarization-induced gene, KID-1, in a rat pheochromocytoma cell line (PC12 cells) (21). The Pim-3 gene is mapped to 22q13 (22) and encodes a protein of 326 amino acids

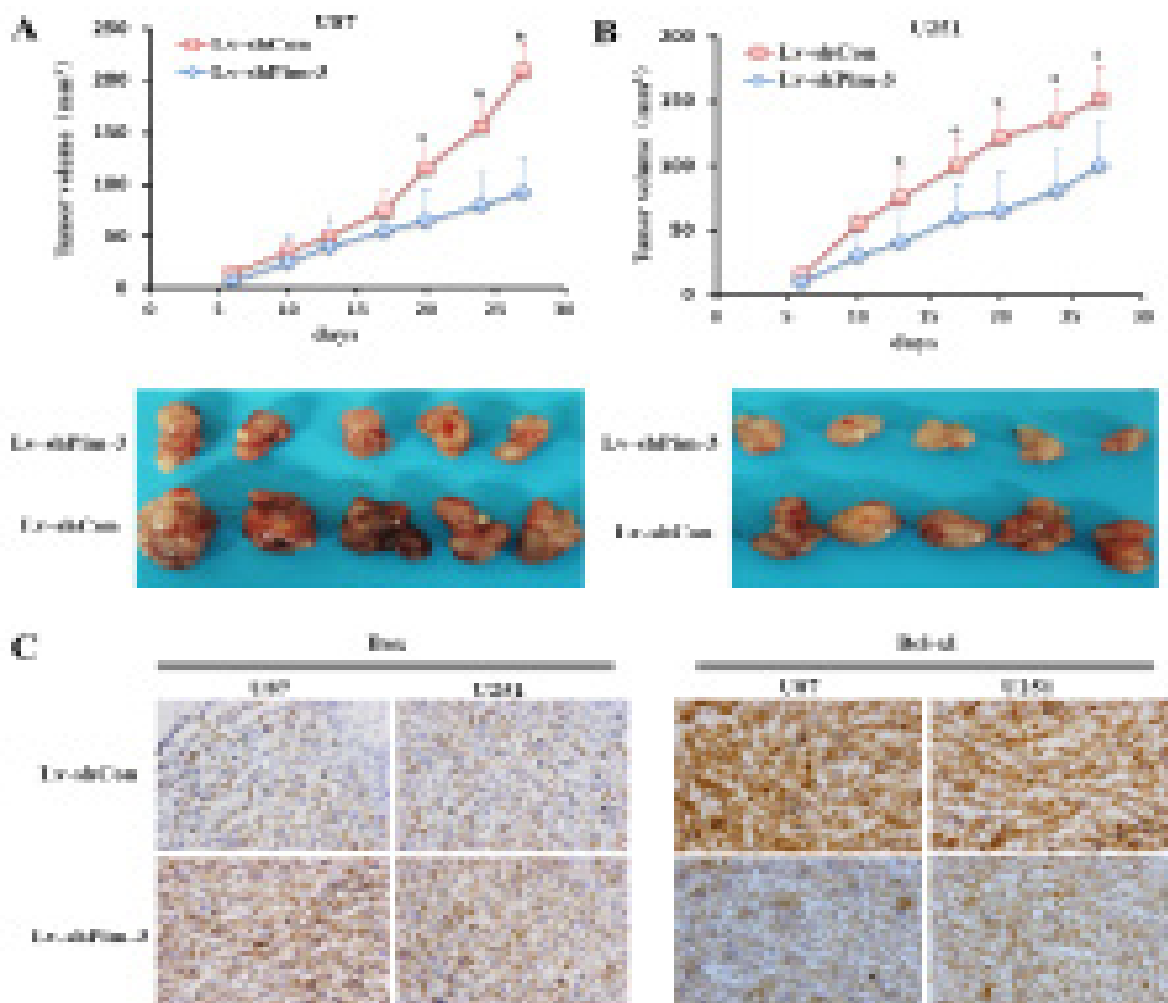


Figure 6. Pim-3 inhibition prevented the growth of tumor xenografts *in vivo*. Tumor volume was periodically monitored in nude mice that were injected with U87 (A, upper panel) or U251 cells (B, upper panel). Cells were infected with Lv-shCon or Lv-shPim-3 before injecting them into mice. Tumors were dissected on day 28 (A and B, lower panels), and analyzed by immunohistochemistry. Pro-apoptotic Bax increased, whereas anti-apoptotic Bcl-xl decreased in response to Pim-3 knockdown in both U87 cells and U251 xenografts (C). Data are presented as mean \pm SD. * $P < 0.05$.

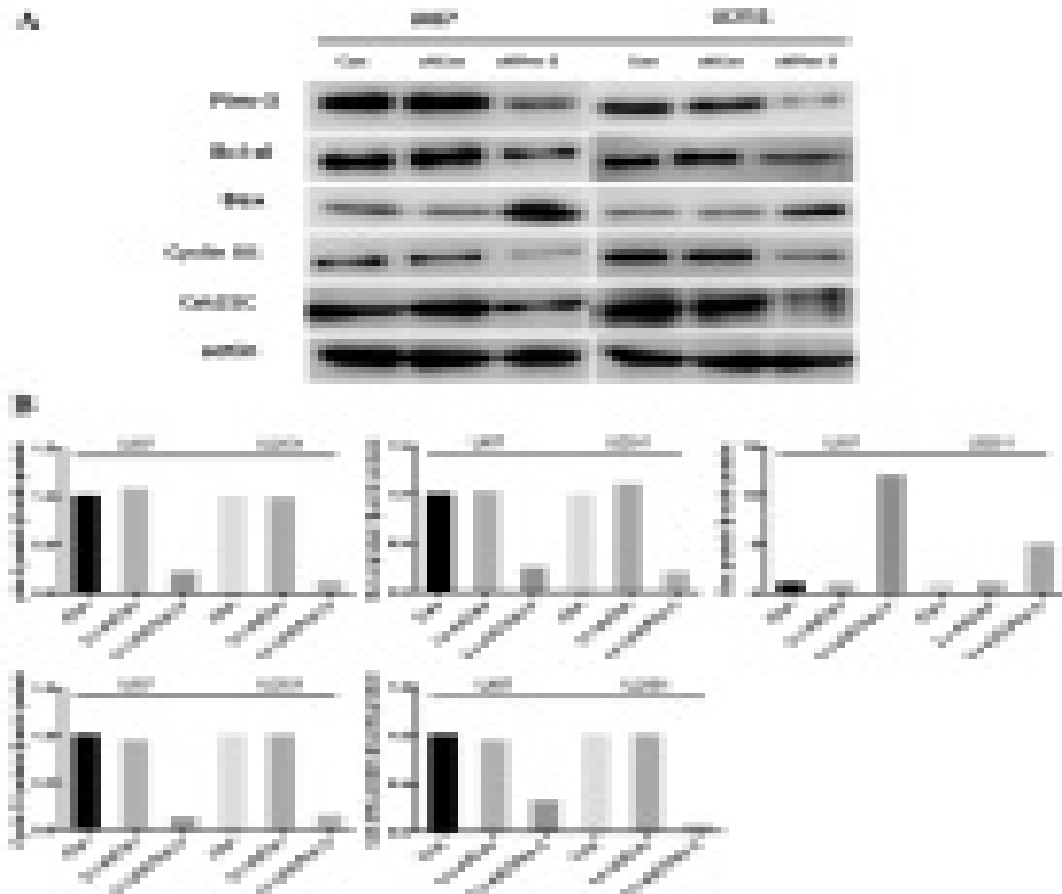


Figure 7. Effects of Pim-3 knockdown on cell cycle regulators and apoptosis-related proteins in U87 and U251 glioblastoma cells. (A) The expression levels of apoptosis-related proteins (Bcl-xl and Bax) and cell cycle regulators (cyclin D1 and Cdc25C) were analyzed by Western blot in uninfected, Lv-shCon infected, and Lv-shPim-3 infected U87 and U251 glioma cells. (B) the expression levels of Pim-3, Bcl-xl, Bax, cyclin D1, Cdc25C and β -actin were quantified using NIH ImageJ software, Pim-3/ β -actin, Bcl-xl/ β -actin, Bax/ β -actin, cyclin D1/ β -actin and Cdc25C/ β -actin ratios were calculated for each cell line.

with a molecular weight of approximately 35 kDa (23). Normal adult endoderm-derived organs including liver, pancreas, colon, and stomach, express very low levels of Pim-3; however, the premalignant and malignant lesions of these organs have enhanced expression of Pim-3 (13, 17, 23, 24). Multiple studies have shown that aberrant Pim-3 expression can occur in the early phase of carcinogenesis. For example, higher levels of Pim-3 protein are detected in regenerative nodules and adenomatous hyperplasia, lesions with precancerous potential, than in HCC cells (23). Another example comes from adenoma tissues, where Pim-3 protein is detected with a higher incidence than in adenocarcinoma tissues in the colon and stomach (17, 24). In our study, we found that Pim-3 was also highly expressed in the human glioblastoma cell lines U87MG, U87, and U251. Pim-3 expression was more than that of the other Pim family members, Pim-1 and Pim-2 (Fig. 1). Regulatory mechanisms that contribute to Pim-3-related tumorigenesis vary in distinct tumors and may even be different in the same type of tumor. A previous study revealed that Pim-3 could be upregulated by the Ewing sarcoma breakpoint region-1/E26 transformation specific (EWS/ETS) fusion proteins (25). In addition, the transcription factor ETS-1 can induce aberrant Pim-3 expression in human pancreatic cancer cells (14). Moreover, translationally controlled tumor protein (TCTP) enhances stability of Pim-3 in pancreatic cancer to simultaneously promote cell-cycle progression and prevent apoptosis (26). In murine embryonic stem cells, Pim-3 expression is also upre-

gulated by leukemia inhibitory factor/gp130-dependent signaling (27). Despite several studies on the mechanisms that contribute to Pim-3-regulated tumorigenesis, the molecular mechanism underlying aberrant Pim-3 expression in glioblastoma still deserves further investigation.

Pim-3 can prevent apoptosis and promote cell survival and protein translation, thereby enhancing proliferation of various types of normal and malignant cells. Pim-3 ablation by RNA interference inhibited cell proliferation and enhanced apoptosis in human hepatoma, pancreatic, and colon cancer cell lines (13, 17, 23). Consistent with previous reports, we too observed that knockdown of Pim-3 via shRNA resulted in a decrease in cell proliferation, an induction of cell cycle arrest in G0/G1 phase, and an increase in apoptosis in the glioblastoma cells *in vitro*. Unphosphorylated proapoptotic protein Bad binds and inactivates the antiapoptotic family members, primarily Bcl-xl, thus promoting apoptosis. Enforced expression of Pim-3 increases the amount of Bad phosphorylation at Ser¹¹² and impairs its binding to Bcl-xl, resulting in apoptosis resistance (13, 17). In D-galactosamine-sensitized rats that are given lipopolysaccharide, Pim-3 gene transduction protects against hepatic failure by increasing Bcl-2 expression and dampening caspase-3 activation (28). In addition, Pim-3-transgenic hepatocytes derived from mouse also enhance phosphorylation of Bad and accelerate cell cycle progression (16). Pim-3 shows a high sequence identity with Pim-1 even in their kinase domains; there-

fore, they may have similar functions. Cdc25C can actively promote cell cycle progression at the G2M phase. Pim-1 phosphorylates Cdc25C-associated kinase 1 (CTAK1)—a potent inhibitor of Cdc25C—and inhibits its activity to eventually advance the cell cycle (29). In this study, knockdown of Pim-3 via shRNA resulted in decreased Cdc25C and Bcl-x1 expression in glioblastoma cells. These observations indicate the molecular mechanisms underlying the effect of Pim-3 on proliferation and apoptosis in glioblastoma cells.

In conclusion, this is the first report elucidating the key role of Pim-3 in growth and apoptosis of glioblastoma cells. The inhibitors of Pim family showed positive therapeutic effects against human pancreatic cancer in xenograft models *in vivo* without causing any major adverse effects (30). Therefore, the findings of this study could be useful for the development of targeted glioblastoma drug therapy.

References

1. Furnari, F. B., Fenton, T., Bachoo, R. M., Mukasa, A., Stommel, J. M., Stegh, A., Hahn, W. C., Ligon, K. L., Louis, D. N., Brennan, C., Chin, L., DePinho, R. A. and Cavenee, W. K., Malignant astrocytic glioma: genetics, biology, and paths to treatment. *Genes Dev* 2007, **21**: 2683-2710. doi: 10.1101/gad.1596707.
2. Kast, R. E., Boockvar, J. A., Bruning, A., Cappello, F., Chang, W. W., Cvek, B., Dou, Q. P., Duenas-Gonzalez, A., Efferth, T., Focosi, D., Ghaffari, S. H., Karpel-Massler, G., Ketola, K., Khoshnevisan, A., Keizman, D., Magne, N., Marosi, C., McDonald, K., Munoz, M., Paranjpe, A., Pourgholami, M. H., Sardi, I., Sella, A., Srivenugopal, K. S., Tuccori, M., Wang, W., Wirtz, C. R. and Halatsch, M. E., A conceptually new treatment approach for relapsed glioblastoma: coordinated undermining of survival paths with nine repurposed drugs (CUSP9) by the International Initiative for Accelerated Improvement of Glioblastoma Care. *Oncotarget* 2013, **4**: 502-530.
3. Tanaka, S., Louis, D. N., Curry, W. T., Batchelor, T. T. and Dietrich, J., Diagnostic and therapeutic avenues for glioblastoma: no longer a dead end? *Nat Rev Clin Oncol* 2013, **10**: 14-26. doi: 10.1038/nrclinonc.2012.204.
4. Stupp, R., Mason, W. P., van den Bent, M. J., Weller, M., Fisher, B., Taphoorn, M. J., Belanger, K., Brandes, A. A., Marosi, C., Bogdahn, U., Curschmann, J., Janzer, R. C., Ludwin, S. K., Gorlia, T., Allgeier, A., Lacombe, D., Cairncross, J. G., Eisenhauer, E. and Mirimanoff, R. O., Radiotherapy plus concomitant and adjuvant temozolomide for glioblastoma. *N Engl J Med* 2005, **352**: 987-996. doi: 10.1056/NEJMoa043330.
5. Zhou, X., Qian, J., Hua, L., Shi, Q., Liu, Z., Xu, Y., Sang, B., Mo, J. and Yu, R., Geranylgeranyltransferase I promotes human glioma cell growth through Rac1 membrane association and activation. *J Mol Neurosci* 2013, **49**: 130-139. doi: 10.1007/s12031-012-9905-3.
6. Masui, K., Cloughesy, T. F. and Mischel, P. S., Review: molecular pathology in adult high-grade gliomas: from molecular diagnostics to target therapies. *Neuropathol Appl Neurobiol* 2012, **38**: 271-291. doi: 10.1111/j.1365-2990.2011.01238.x.
7. Vlachostergios, P. J., Voutsadakis, I. A. and Papandreou, C. N., The ubiquitin-proteasome system in glioma cell cycle control. *Cell Div* 2012, **7**: 18. doi: 10.1186/1747-1028-7-18.
8. Castro, M. G., Candolfi, M., Kroeger, K., King, G. D., Curtin, J. F., Yagiz, K., Mineharu, Y., Assi, H., Wibowo, M., Ghulam, M. A., Foulad, D., Puntel, M. and Lowenstein, P. R., Gene therapy and targeted toxins for glioma. *Curr Gene Ther* 2011, **11**: 155-180.
9. Vecil, G. G. and Lang, F. F., Clinical trials of adenoviruses in brain tumors: a review of Ad-p53 and oncolytic adenoviruses. *J Neurooncol* 2003, **65**: 237-246. 10. Marsh, J. C., Goldfarb, J., Shafman, T. D. and Diaz, A. Z., Current status of immunotherapy and gene therapy for high-grade gliomas. *Cancer Control* 2013, **20**: 43-48.
11. An, S., Nam, K., Choi, S., Bai, C. Z., Lee, Y. and Park, J. S., Nonviral gene therapy *in vivo* with PAM-RG4/apoptin as a potential brain tumor therapeutic. *Int J Nanomedicine* 2013, **8**: 821-834. doi: 10.2147/IJN.S39072.
12. Mukaida, N., Wang, Y. Y. and Li, Y. Y., Roles of Pim-3, a novel survival kinase, in tumorigenesis. *Cancer Sci* 2011, **102**: 1437-1442. doi: 10.1111/j.1349-7006.2011.01966.x.
13. Li, Y. Y., Popivanova, B. K., Nagai, Y., Ishikura, H., Fujii, C. and Mukaida, N., Pim-3, a proto-oncogene with serine/threonine kinase activity, is aberrantly expressed in human pancreatic cancer and phosphorylates bad to block bad-mediated apoptosis in human pancreatic cancer cell lines. *Cancer Res* 2006, **66**: 6741-6747. doi: 10.1158/0008-5472.CAN-05-4272.
14. Li, Y. Y., Wu, Y., Tsuneyama, K., Baba, T. and Mukaida, N., Essential contribution of Ets-1 to constitutive Pim-3 expression in human pancreatic cancer cells. *Cancer Sci* 2009, **100**: 396-404. doi: 10.1111/j.1349-7006.2008.01059.x.
15. Chang, M., Kanwar, N., Feng, E., Siu, A., Liu, X., Ma, D. and Jongstra, J., PIM kinase inhibitors downregulate STAT3(Tyr705) phosphorylation. *Mol Cancer Ther* 2010, **9**: 2478-2487. doi: 10.1158/1535-7163.MCT-10-0321.
16. Wu, Y., Wang, Y. Y., Nakamoto, Y., Li, Y. Y., Baba, T., Kaneko, S., Fujii, C. and Mukaida, N., Accelerated hepatocellular carcinoma development in mice expressing the Pim-3 transgene selectively in the liver. *Oncogene* 2010, **29**: 2228-2237. doi: 10.1038/onc.2009.504.
17. Popivanova, B. K., Li, Y. Y., Zheng, H., Omura, K., Fujii, C., Tsuneyama, K. and Mukaida, N., Proto-oncogene, Pim-3 with serine/threonine kinase activity, is aberrantly expressed in human colon cancer cells and can prevent Bad-mediated apoptosis. *Cancer Sci* 2007, **98**: 321-328. doi: 10.1111/j.1349-7006.2007.00390.x.
18. Wang, C., Li, H. Y., Liu, B., Huang, S., Wu, L. and Li, Y. Y., Pim-3 promotes the growth of human pancreatic cancer in the orthotopic nude mouse model through vascular endothelium growth factor. *J Surg Res* 2013, **185**: 595-604. doi: 10.1016/j.jss.2013.06.004.
19. Liu, B., Wang, Z., Li, H. Y., Zhang, B., Ping, B. and Li, Y. Y., Pim-3 promotes human pancreatic cancer growth by regulating tumor vasculogenesis. *Oncol Rep* 2014, **31**: 2625-2634. doi: 10.3892/or.2014.3158.
20. Bittker, J. A., Weiwer, M., Wei, G., Germain, A., Brown, E., Dandapani, S., Munoz, B., Palmer, M., Golub, T. and Schreiber, S. L., Discovery of Inhibitors of Anti-Apoptotic Protein A1., 2010.
21. Feldman, J. D., Vician, L., Crispino, M., Tocco, G., Marcheselli, V. L., Bazan, N. G., Baudry, M. and Herschman, H. R., KID-1, a protein kinase induced by depolarization in brain. *J Biol Chem* 1998, **273**: 16535-16543.
22. Nawijn, M. C., Alendar, A. and Berns, A., For better or for worse: the role of Pim oncogenes in tumorigenesis. *Nat Rev Cancer* 2011, **11**: 23-34. doi: 10.1038/nrc2986.
23. Fujii, C., Nakamoto, Y., Lu, P., Tsuneyama, K., Popivanova, B. K., Kaneko, S. and Mukaida, N., Aberrant expression of serine/threonine kinase Pim-3 in hepatocellular carcinoma development and its role in the proliferation of human hepatoma cell lines. *Int J Cancer* 2005, **114**: 209-218. doi: 10.1002/ijc.20719.
24. Zheng, H. C., Tsuneyama, K., Takahashi, H., Miwa, S., Sugiyama, T., Popivanova, B. K., Fujii, C., Nomoto, K., Mukaida, N. and Takano, Y., Aberrant Pim-3 expression is involved in gastric adenoma-adenocarcinoma sequence and cancer progression. *J Cancer Res Clin Oncol* 2008, **134**: 481-488. doi: 10.1007/s00432-007-0310-1.
25. Deneen, B., Welford, S. M., Ho, T., Hernandez, F., Kurland, I.

and Denny, C. T., PIM3 proto-oncogene kinase is a common transcriptional target of divergent EWS/ETS oncoproteins. *Mol Cell Biol* 2003, **23**: 3897-3908.

26. Zhang, F., Liu, B., Wang, Z., Yu, X. J., Ni, Q. X., Yang, W. T., Mukaida, N. and Li, Y. Y., A novel regulatory mechanism of Pim-3 kinase stability and its involvement in pancreatic cancer progression. *Mol Cancer Res* 2013, **11**: 1508-1520. doi: 10.1158/1541-7786.MCR-13-0389.

27. Aksoy, I., Sakabedoyan, C., Bourillot, P. Y., Malashicheva, A. B., Mancip, J., Knoblauch, K., Afanassieff, M. and Savatier, P., Self-renewal of murine embryonic stem cells is supported by the serine/threonine kinases Pim-1 and Pim-3. *Stem Cells* 2007, **25**: 2996-3004. doi: 10.1634/stemcells.2007-0066.

28. Liu, L. M., Zhang, J. X., Wang, X. P., Guo, H. X., Deng, H. and

Luo, J., Pim-3 protects against hepatic failure in D-galactosamine (D-GalN)-sensitized rats. *Eur J Clin Invest* 2010, **40**: 127-138. doi: 10.1111/j.1365-2362.2009.02235.x.

29. Bachmann, M., Hennemann, H., Xing, P. X., Hoffmann, I. and Moroy, T., The oncogenic serine/threonine kinase Pim-1 phosphorylates and inhibits the activity of Cdc25C-associated kinase 1 (C-TAK1): a novel role for Pim-1 at the G2/M cell cycle checkpoint. *J Biol Chem* 2004, **279**: 48319-48328. doi: 10.1074/jbc.M404440200.

30. Li, Y. Y., Wang, Y. Y., Taniguchi, T., Kawakami, T., Baba, T., Ishibashi, H. and Mukaida, N., Identification of stemonamide synthetic intermediates as a novel potent anticancer drug with an apoptosis-inducing ability. *Int J Cancer* 2010, **127**: 474-484. doi: 10.1002/ijc.25048.